Modeling Cutting Process Nonlinearity for Stability Analysis — Application to Tooling Selection for Valve-Seat Machining

William J. Endres
Dept. of Mech. Eng. – Eng. Mechanics
Michigan Technological University
Houghton, MI 49931-1295

Ming Loo
Advanced Manuf. Technology Dev.
Ford Motor Company
Dearborn, MI

Abstract

When simulating most industrially used machining processes semi-empirical process force models are often used to relieve the computational burden of other modeling approaches, like FEA or slip-line fields. While the exact forms of these models vary somewhat, they typically model the process force as proportional to the uncut chip area through the specific energy. The specific energy is typically modeled in some power-law form with uncut chip thickness, among other variables. This approach yields force predictions to within ten percent or better. However, stability depends on the gradient of the process force with respect to uncut chip thickness, not the force value itself. A new model form is formulated to better capture the force-uncut chip thickness gradient. It is used to select the best edge preparation for each tooth in valve-seat machining where the range of uncut chip thickness seen across the three cutting teeth is very large, requiring the process force gradient to be well predicted across that entire range.

1 INTRODUCTION

Machining stability, or instability, is a product of the coupling of the machine-tool system structure and the machining process. Efforts to avoid instability/chatter problems during the design of a machine tool often focus on the structure by increasing stiffness and or damping in its various elements, such as the machine tool, fixturing and tooling. Increasing *dynamic stiffness*, which is affected by both static stiffness and damping, is the main strategy with the spindle, slide interfaces and tool-clamping interfaces as primary targets. However, increased dynamic stiffness usually comes at increased expense through a larger machine-tool structure and subsequently larger spindles and slides, and consequently larger drives to accelerate those higher-mass components. For that reason, there is much to gain by scientifically selecting tooling, at the design stage, that will enhance stability toward relaxing the demands on the structural requirements.

Despite efforts made during design, the existence of stability problems in practice are typically not known until the machine tool, fixturing and tooling have been built and integrated in the tryout phase. At that point, a solution must be found quickly and at the least out-of-pocket cost. Changing structural elements of the machine tool and fixturing is not an attractive option due to the high cost and lead-time. A more attractive option is to adjust the machine settings. For instance, it is well known that spindle speed can be set, in the high-speed regime, to take advantage of stability peaks. There is also a general rule of thumb that increasing feed will improve stability [1], which is supported by process mechanics through what is known as the ‘size effect’ [2].

However, there are some caveats to relying on adjustment of machine settings to solve stability problems. For instance, in transfer-line settings the drives on some stations are not even capable of such adjustments. And, for stations where spindle speed and federate can be adjusted, any changes must keep the station within the system cycle time. For machining centers, on the other hand, increasing cycle time on one tool can possibly be made up by decreasing cycle time on another. In this case, adjustment of machine settings may be a viable approach, in which case it is advantageous to understand the sensitivity of stability to changes in feed and speed and their interaction with tooling parameters.

Despite the aforementioned methods to solve stability problems, it is well accepted that it is typically easier and less costly to replace tooling.

As a result, practicing engineers most often target 'tooling' as a solution to chatter problems [3]. Reducing tool overhangs and stiffening the tool-chuck interfaces may be a strategy when dynamic testing suggests those as weak links. However, the gross geometry of the tool — lead angle, corner radius and rake angles, for example — is the more typical target as a means to solve instability problems [3]. On the other hand, the small-scale geometry like edge preparation is rarely considered to solve such problems [3].

To scientifically target tool geometry towards solving or avoiding instability problems, process force models must accurately capture the effects that tooth geometry and machine settings have on the process attributes that affect stability. The effects of gross tool geometry, like corner radius and lead angle, are well understood to affect the directions of forces. Some recent studies have formulated geometrical models that capture the contribution of these parameters to average uncut chip thickness and subsequently to the nonlinear size effect [4]. Various forms of process force models, including the power-law form used by Ozdoganlar and Endres [4], have demonstrated consistently to provide a force-prediction accuracy of 10% error across ranges of uncut chip thickness [5, 6, 7]. However, the stability problem is not affected by the force itself, but rather by the gradient of the force relative to the dynamic displacements as manifested through their effects on process geometry, such as uncut chip thickness. Therefore, from the perspective of stability analysis, it is more critical to accurately model the force gradients than it is to accurately model the force level.

The work presented here studies the capability of existing process force models to accurately capture the *gradient* of the force with respect to uncut chip thickness toward proposing an alternate model form that more consistently captures this gradient while also providing equivalently good predictions of force level. It is well known that small-scale tooth geometry — edge preparation — and its size relative to the uncut chip thickness, is explicitly related to the nonlinear size effect. Therefore, while it is not the intent of this work to model the effect of edge preparation, it is varied in the experiments as a means to exercise the models beyond varying uncut chip thickness alone as motivated by selecting improved tooling for valve-seat machining. As will be seen, though based on less data than desired in hindsight, some materials appear to exhibit a very interesting and counterintuitive gradient characteristic when using edge-radiused (honed) tools.

2 ASSESSMENT OF TRADITIONAL FORCE MODELING FOR STABILITY ANALYSIS

Early work on the application of stability analysis led to the concept of Dynamic Cutting Force Coefficients (DCFCs). This approach intended to provide a complete characterization of the coupled process and machine-tool dynamics into four coefficients [8, 9, 10]. The four coefficients account for process stiffness and damping related to both the primary and regenerative displacement effects. Each set of coefficients is specific to not only the work material at hand, but also the machine tool and tooling at hand. The approach has the potential of very comprehensively accounting for the dynamics of the machine-tool system. However, it requires not only substantial testing, but also an existing machine tool and tooling.

Another approach taken by many more recent efforts is to decouple the machine tool and process. The approach makes use of frequency response testing of machine tools or beam theory predictions of tool dynamics along with static process force models [11, 12, 13]. Static force models are extended to the dynamics problem by replacing the static chip area with the dynamic or modulated chip area. To take that a step further, the effect of dynamic displacements that enter through the specific energy portion of the force model has been introduced as well [2, 4]. In the valve-seat machining problem at hand, though a specific machine tool may exist, the specific tooling does not. Therefore, decoupling the tooling and machine-tool characteristics is particularly important — the intent is to select the tooling that will enhance stability irrespective of the machine tool.

To better understand the effect of edge preparation on process nonlinearity and hence stability, tests were conducted using four levels of edge radius, up-sharp (5 μm), 13 μm, 25 μm and 50 μm. Edge radius levels were measured under an optical microscope in the region of the lead edge where the cuts would be made. Uncoated carbide, zero-lead, zero-rake tooling was used to machine a powder metallurgy material at two hardness levels. The materials are used for valve seats and are referred to as Material A (softer) and Material B (harder).

Valve-seat blanks of 25-mm length were mounted in the chuck of a CNC lathe for end-turning under straight-edged orthogonal cutting conditions with the blank's 2-mm wall thickness being the width of cut. Tests at five levels of uncut chip thickness (*h*-levels) were conducted in random order and replicated three times using a fresh cutting edge for each replication. Forces were measured via a Kistler three-component dynamometer in a typical force-testing arrangement. The charge amplifier ranges were set to 500 N/volt so that the low forces being measured (20 N minimum) consumed most of the range, ultimately maximizing the analog-to-digital conversion resolution (< 0.02 N, or 1/1000 of the minimum measurement). No chatter was observed, based on inspection of the machined surface at the end of each test. Any elastic spring-back or work hardening under the edge is experienced in the subsequent revolution and are natural occurrences in machining as the tool feeds to remove a previously cut surface from one revolution/tooth-pass in the past.

2.1 Force Prediction

It is well accepted that the machining force components vary proportionally with the chip area *a* as

$$F_\bullet = u_\bullet a \,, \tag{1}$$

where $u_\bullet$ is the specific energy for the cutting ($\bullet$ = '*C*') or thrust ($\bullet$ = '*T*') direction. The specific energy is typically modeled to include the nonlinear effects of cutting speed *V*, uncut chip thickness *h*, as well as normal rake angle, γ_n. A model form that has gained some popularity is

$$u_\bullet = b_{0_\bullet} h^{b_{h_\bullet}} V^{b_{V_\bullet}} (1-\sin\gamma_n)^{b_{\gamma_\bullet}}, \bullet = C, T \,. \tag{2}$$

The uncut chip thickness nonlinearity is the mathematical representation of size effect. The power-law form was suggested by Sabberwal [14] and has been used by many since. For dynamic analysis, it is common to directly extend this static force model so that the dynamic or modulated force is modeled to be proportional to the dynamic or modulated chip area, i.e.,

$$F(t)_\bullet = u_\bullet(t) a(t) \,. \tag{3}$$

The dynamic chip area embodies one of the primary effects of the dynamic displacements. Other effects of dynamic displacements enter through the specific energy; hence, it is written in Eq. (3) as $u(t)$ — an explicit function of time (actually, state). For instance, the uncut chip thickness, being one of the dimensions of the chip area, introduces an additional effect of dynamic displacements through the specific energy (Eq. (2)). The cutting speed can be affected by dynamic displacements in that direction while the rake angle can be affected by rotational displacements; however, these effects are typically small (second order) relative to those that enter through the uncut chip thickness and chip area. Therefore, for dynamic analysis it is possible and customary to group the cutting speed and rake angle effects of Eq. (2) into a leading constant $u_{c_\bullet}$ as

$$u_\bullet(t) = u_{c_\bullet} h(t)^{b_{h_\bullet}} \,, \tag{4}$$

where

$$u_{c_\bullet} = b_{0_\bullet} V^{b_{V_\bullet}} (1-\sin\gamma_n)^{b_{\gamma_\bullet}}, \bullet = C, T \,.$$

Another approach used by Hanna and Tobias [15] directly modeled the unit force (force per unit width of cut) versus uncut chip thickness as a second-order polynomial. They too (implicitly) lumped the speed and rake angle effects into a leading constant due to their relative unimportance in the dynamics/stability problem.

The effect of uncut chip thickness on the unit process force is shown in Figures 1-2[1] for the up-sharp tools and the largest edge radius (50 μm). Included with the experimental data is the unit force obtained using a least-square fit of the power-law form of specific energy given in Eq. (4) and a second-order polynomial for the unit force, like that used by Hannah and Tobias [15]. The model fits were made using the minimum number of *h*-levels required for the fit, i.e., two levels for the power law, being linear in the log space, and three levels for the second-order polynomial. In most cases, either model does fairly well to predict the forces, exhibiting errors of ±20% at most, and typically closer to ±10%. In particular, the traditional specific-energy power law does well considering only the lowest and highest *h*-levels were used to fit the model, compared to the second-order polynomial that requires four of the five *h*-levels in the data set.

[1] In these and subsequent figures, 'SE' indicates that the empirical portion of the force model is the specific energy, from which the unit force is computed by multiplying by the uncut chip thickness, and 'UF' indicates that the empirical portion of the force model constitutes the entire model, i.e., the unit force itself.

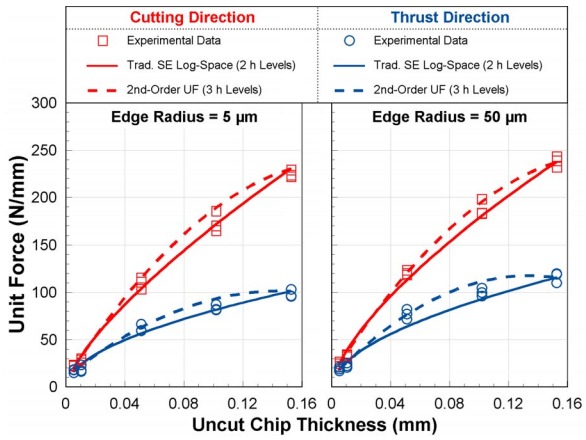

Figure 1: Unit force vs. uncut chip thickness for Material A — up-sharp (left) and 50 µm edge radius (right).

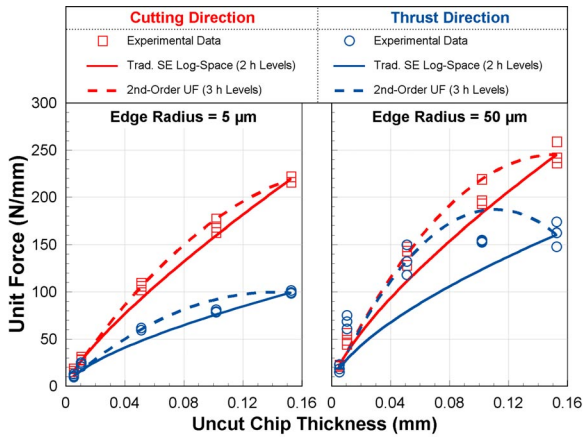

Figure 2: Unit force vs. uncut chip thickness for Material B — up-sharp (left) and 50 µm edge radius (right).

These error percentages are on par with model predictions noted in a variety of past studies that have applied the specific-energy power-law model to various processes.

2.2 Stability Prediction

As noted earlier, many have studied the stability of machining for numerous types of processes. Consider the basic case of straight-edged orthogonal cutting often considered as representative of turning or boring with a zero corner radius. A schematic of this classical case is shown in Figure 3, and on a tooth-wise basis is quite representative of valve-seat machining. To avoid distraction from the focus on force modeling, stability analysis is restricted here to this case. It is considered to be an approximate representation of the valve-seat machining process that provides for a good relative

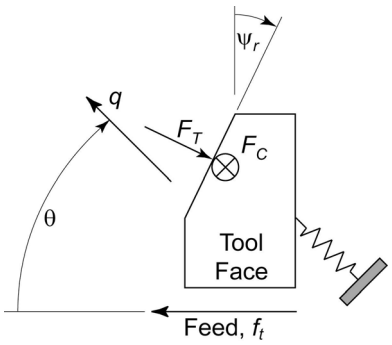

Figure 3: Basic dynamics of straight-edged orthogonal machining.

assessment of force model alternatives and, later, tooling alternatives.

Stability Limit Solution

The dominant dynamic mode q is oriented at angle θ relative to the feed direction and the cutting edge is oriented relative to the feed-normal direction by the lead angle ψ_r. In this case the cutting force F_C acts perpendicular to the chip area plane and, hence, has no substantive effect on the modal displacement. The thrust force component, F_T, lies in the chip area plane and, hence, has a direct effect on the modal displacement. For this case the equation of motion for the closed-loop system is

$$S\left(q(t), q(t), \ldots, q^{(m)}(t)\right) = F_q \,, \tag{5}$$

where $S\left(q(t), \dot{q}(t), \ddot{q}(t) \ldots, q^{(m)}(t)\right)$ is an m^{th}-order differential equation representing the structure's dynamics. For example,

$$S\left(q(t), \dot{q}(t), \ddot{q}(t), \ldots, q^{(m)}(t)\right) = m\ddot{q}(t) + c\dot{q}(t) + kq(t)$$

for a second-order system. The modal force acting in the q direction is

$$F_q(t) = -F_T(t)\cos(\theta - \psi_r) \,. \tag{6}$$

Introducing the process force as computed via the specific energy model of Eq. (4), where the uncut chip thickness, being measured in the chip area plane and normal to the cutting edge is

$$h(t) = \left(q(t) - q(t - T_t)\right)\cos(\theta - \psi_r) \,, \tag{7}$$

Eq. (5) becomes

$$S\left(q(t), q(t), \ldots, q^{(m)}(t)\right) = -u_{c_T} h^{b_{hT}} \cdot wh\cos^2(\theta - \psi_r) \,, \tag{8}$$

where T_t is the regenerative delay.

To apply linear frequency-domain stability techniques, Eq. (8) must be linearized with respect to the state variable(s). A strict and formal linearization of this equation of motion with respect to the state variable $q(t)$, and likewise $q(t - T_t)$, due to the delay term, would evolve to an infinite order in the system. However, it has been shown that linearization of the process force alone with respect to $h(t)$ as opposed to $q(t)$ and $q(t - T_t)$ provides the appropriate stability result. This was confirmed through comparison of analytical results to nonlinear numerical time-domain simulations (Endres, 1996). The result of the linearization, after ignoring the resulting static or zero-h force is

$$S\left(q(t), q(t), \ldots, q^{(m)}(t)\right) = -u_{c_T}\left(b_{h_T}+1\right)h^{b_{h_T}} \cdot w\cos^2(\theta-\psi_r), \qquad (9)$$

where the equilibrium uncut chip thickness h_e is $f_t\cos\psi_r$, f_t being the nominal feed per tooth.

Now, applying the usual harmonic response presumption, rearranging and solving for the limiting width of cut, the final result is

$$w_{lim} = \frac{1}{-2u_{c_T}\left(b_{h_T}+1\right)h_e^{\,b_{h_T}}\cos^2(\theta-\psi_r)} \times \frac{1}{\mathrm{Re}\left\langle G(j\omega_c)\right\rangle}, \qquad (10)$$

where $G(j\omega_c)$ is the frequency-response function of the structure evaluated at the chatter frequency ω_c.

Force Model Gradient Assessment

The term $u_{c_T}\left(b_{h_T}+1\right)h_e^{\,b_{h_T}}\cos(\theta-\psi_r)$ in the denominator of Eq. (10) is clearly the slope of the linearization introduced in Eq. (9), or rather the gradient of the unit force F_q/w with respect to uncut chip thickness. This is where the traditional process force models, shown above to fair well in terms of force prediction, break down. As shown in Figures 4 and 5, these model forms do poorly in terms of representing the unit-force gradient with respect to uncut chip thickness. In most cases, the power-law specific energy form does better, but still exhibits errors ranging from ±25% **at best** to more typical ones around 50-100% and even some in excess of 200%.

Some of the very extreme errors arise at the lower uncut chip thicknesses as a result of a

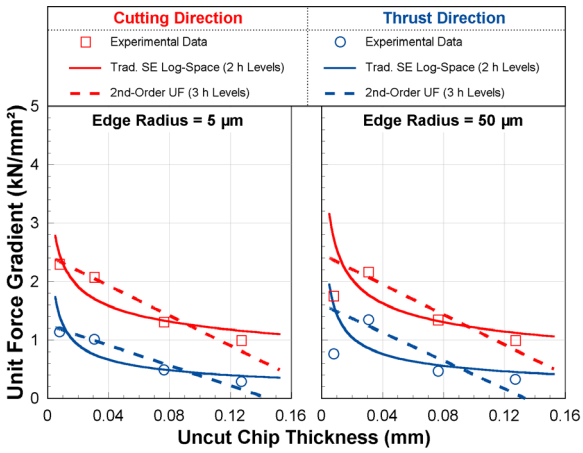

Figure 4: Unit-force gradient vs. uncut chip thickness for Material A, via derivative of traditional unit force models of Figure 1.4

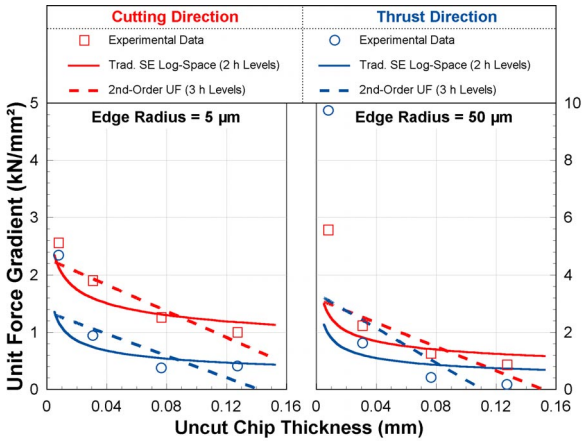

Figure 5: Unit-force gradient vs. uncut chip thickness for Material B, via derivative of traditional unit force models of Figure 2.

characteristic seen here that is both counterintuitive and not previously noted. Specifically, the larger edge radius case (right plot) of Figure 4 shows that the gradient, though increasing with decreasing uncut chip thickness as we would expect from the traditional size effect concept, actually drops at the lowest h-level. While more data is needed to assure that this is neither a fluke nor experimental error, it does consistently occur for many of the edge-radiused tools, as well as for chamfered tools, for the softer Material A. On the other hand, cases of higher edge radius for the harder Material B exhibit an exorbitant increase in unit force gradient at the lowest h-level (see right plot of Figure 5).

Neither model form can be expected to capture these characteristics at low uncut chip thickness.

However, one could argue that these values of uncut chip thickness are very small and machining typically does not take place at such small feeds. But, such situations are in fact seen in ultra-precision and hard machining that often exhibit an edge preparation that is substantial in size relative to the uncut chip thickness. These conditions are also seen at conventional feeds and in conventional processes. For instance, small uncut chip thicknesses are also seen with the high lead angles ($h = f_t \cos\psi_r$) inherent to valve-seat machining as well as when dwells are imposed at the end of a cut to meet tight dimensional tolerances, such as in valve-seat machining, among others.

To summarize, there is clearly room for improvement in the area of semi-empirical force modeling to better characterize the unit-force gradient that embodies the main effect of the process force on the stability problem. The power-law specific energy-based model, which was developed to predict forces while accounting for size effect — the nonlinear dependence of force on uncut chip thickness — falters mainly at low uncut chip thicknesses and exhibits errors in the range of ±30-40% at moderate uncut chip thicknesses. The second-order polynomial form, which was in fact proposed by Hanna and Tobias [15] to represent the size effect for use in stability analysis, performs even worse for these data and additional tests for Materials A and B using chamfered tools.

3 A MODIFIED SEMI-EMPIRICAL FORCE MODEL

With the above findings as motivation, it is desired to formulate a semi-empirical model form that better represents the low-*h* surge, the moderate-*h* decay, and high-*h* asymptote as general characteristics of the unit-force gradient. The true existence of a low-*h* drop-off, as seen for Material A, is in question due to an insufficient amount of data, i.e., only one *h*-level being on the downside of the peak. Therefore, this characteristic is left as an observation and no attempt is made to accommodate it in the proposed model. Therefore the remainder of the paper will address Material B and its low-*h* surge, moderate-*h* decay, and high-*h* asymptote.

The above results show that models able to represent the force to reasonable levels of accuracy are not assured to well characterize the gradient. However, a model fit to the gradient should well represent its integral. For that reason and the fact that the gradient graphs show much more sensitivity to changes in uncut chip thickness than does the unit force, a new model is proposed/formulated as a gradient model from which a unit-force model can be derived through its integration.

In assessing the model, it will be fit in its gradient form (to computed/derived gradient data) as well as in its integrated unit-force form (to measured force data) to see which manner of fitting is preferred. This exercise is important since the model is formulated for the gradient, whereas fitting it to measured forces would likely be preferred since it is the force that is measured in testing, not the gradient. Computing the gradient could well require more *h*-levels and replications to make the results robust to effects of noise in the force measurements that are amplified upon differentiation, as is the case when differentiating any 'real' signal that contains noise.

3.1 The Model Form

One might expect the low-*h* surge to be well modeled via the derivative of the power-law specific energy model, that is

$$\frac{d}{dh}\left(F_\bullet \big/ w\right) = -u_{c_\bullet}\left(b_{h_\bullet}+1\right)h_e^{\,b_{h_\bullet}}, \quad \bullet = C, T,$$

or any power-law form for that matter. The data show that is not the case. There are three consequences to the fact that in order to achieve the moderate-*h* decay, the uncut chip thickness exponent must be negative. They are:

1. As uncut chip thickness approaches zero, the gradient of the power law does become large; in fact, it approaches infinity. However, to match the moderate-*h* decay rate, the gradient more abruptly approaches infinity than the actual data. Furthermore, unlike specific energy by definition, there is no reason to expect the force gradient to be infinite at zero uncut chip thickness.
2. The high-*h* asymptote is prescribed to be zero. However, this is easily overcome by adding a constant as a third parameter in the model to alleviate this.
3. As a side note in the case that the low-*h* drop-off is later shown to truly exist, since the power-law model approaches infinity in the low-*h* regime, there is no function that could successfully scale it down to produce the low-*h* drop-off.

Another candidate is a log function. It has a non-zero large-h asymptote to which a constant could be added to get the appropriate value, but it too approaches infinity at zero uncut chip thickness and, hence, suffers the same shortcomings described in points 1 and 3 above.

The chosen candidate is an exponential with an added constant to obtain a non-zero high-h asymptote. It also provides more flexibility in controlling the decay rate. Finally, since the exponential of zero is finite, it both makes more physical sense than an infinite zero-h gradient, and exhibits the potential to be scaled down to achieve the low-h drop-off if it exists. The resulting gradient/model function used here has three parameters:

$$\frac{d}{dh}\left(F/w\right) = b_1 + b_2 \exp(b_3 h)\,. \qquad (11)$$

The parameters provide the following characteristics to the function:

- b_1 is the high-h asymptote.
- b_2, along with b_1, is the low-h surge height.
- b_3 is the moderate-h decay rate.

The unit-force function is then found by integrating the gradient function. The result is

$$F/w = \int \left[b_1 + b_2 \exp(b_3 h)\right] dh$$
$$= b_1 h + \frac{b_2}{b_3}\exp(b_3 h) + b_4\,, \qquad (12)$$

where b_4 is the constant of integration.

3.2 Force Gradient

Unit-force gradients were computed from the measured unit force data as follows. For N_h h-levels in the force data, there are $N_h - 1$ h-levels in the gradient data. The gradient at $h = (h_i + h_{i+1})/2$ is $(F_{i+1} - F_i)/(h_{i+1} - h_i)$, where F_i and F_{i+1} are the forces, averaged over all replications, at uncut chip thickness h_i and h_{i+1}, respectively. Averaging the force over replications provides for some averaging out of natural experimental error/noise in the force measurements.

Models were fit using Microsoft Excel® and its *Solver* add-in taking care to start with sensible initial values for the parameters to assure a sensible converged set of parameters. Results are shown in Figure 6. The solid curves are obtained by inserting into the gradient function the parameters computed by fitting the gradient function (Eq. (11)) to the computed gradient data. The dashed curves are obtained by inserting into the gradient function the parameters computed by fitting the unit-force function (Eq. (12)) to the measured force data. There is no advantage to having one more h-level in the force data since the unit-force function has one more parameter (the integration constant) than does the gradient function. The graphical display in the figures is evidence that the curves are consistent with the trends, and much improved in comparison to Figure 5. In comparing the two fits, the gradient fits (solid curves) are indeed better.

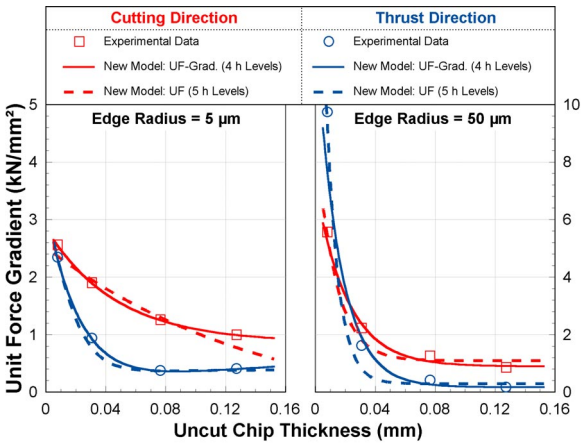

Figure 6: Unit-force gradient vs. uncut chip thickness for Material B; model being fit to both the unit force (UF) and the unit-force gradient (UF-Grad).

The next step is to see how well the gradient and unit force fits compare in terms of predicting the force.

3.3 Force Level

In this case, the curves are switched compared to the gradient evaluation above. That is, the solid curves are obtained by inserting into the unit-force function the parameters computed by fitting the unit-force function (Eq. (12)) to the measured force data; the dashed curves are obtained by inserting into the unit-force function the parameters computed by fitting the gradient function (Eq. (11)) to the computed gradient data. When using the gradient-fit parameters, the fourth parameter of Eq. (12), the integration constant, is computed as the average offset/error between the measured force data and the respective forces computed using the gradient-fit parameters b_1 through b_3. The observation here, seen in Figure 7, is that both approaches do very well in predicting the forces. While the parameters of the unit-force fit work better to predict unit force, they work more poorly for the

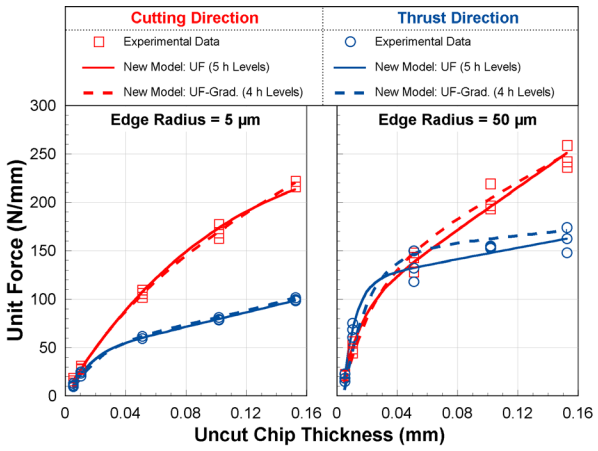

Figure 7 Unit force vs. uncut chip thickness for Material B; model being fit to both the unit force (UF) and the unit-force gradient (UF Grad).

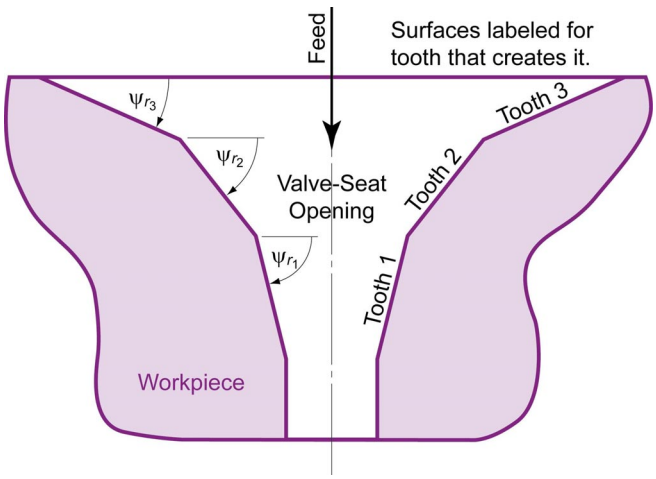

Figure 8: Valve seat cross-section geometry showing tooth that creates each facet.8

gradient predictions than the gradient-fit parameters do for the unit-force predictions. This supports a preference to fit the gradient model to computed gradient data.

4 APPLICATION TO STABILITY OF VALVE-SEAT MACHINING

One of the primary factors that affect machining stability is the direction of the machining force relative to the dynamic modes, which is characterized as *directional factors* [16, 17] or included directly as part of the *oriented transfer function* [18]. These directional factors, the $\cos(\theta - \psi_r)$ in Eq. (6), are not adjustable by selecting tool geometry (ψ_r) in the valve-seat machining problem since the lead angle is dictated by the faceted part geometry, as shown in Figure 8. Therefore, valve-seat machining presents a challenging stability problem, leaving only secondary process parameters to be adjusted.

Past studies [19] have helped to qualitatively understand the machine-tool dynamics part of this problem, including the spindle dynamics and to some degree the tool-clamping dynamics. Realizing further improvements through increased stiffness can become very costly, coming with motor/spindle powers that are 100-200 times the required process cutting power. The reported work was motivated by the prospect of further improving stability through the controllable cutting-tool geometry parameters and machine settings. By focusing on the process rather than the machine tool (spindle, etc.), improvement may be realized for existing processes at a reasonable cost.

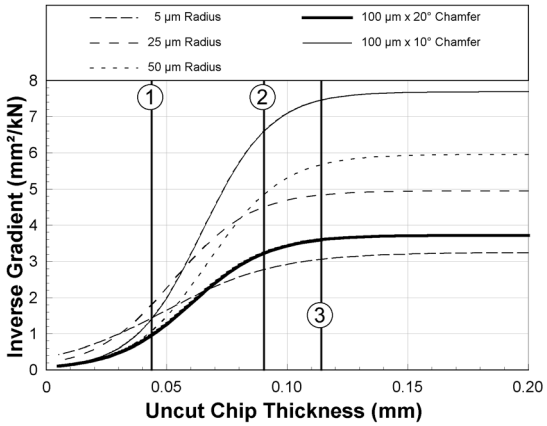

Figure 9: Effect of edge preparation on stability (inverse gradient) for each tooth.

With the above as motivation, and the unit-force gradient characteristics identified and modeled above, the gradient model can be used to compare a variety of edge preparations toward selecting one that should maximize stability. Using representative lead angles of 70°, 45° and 15° for teeth 1, 2 and 3, Figure 9(left) shows the inverse of the gradient computed with the proposed model for an up-sharp tool, two edge-radiused tools and two chamfered tools. The heavy curve is the “baseline” tool over which improvement is desired. The lines labeled as 1, 2 and 3 indicate the uncut chip thickness experienced by that respective tooth as influenced by the lead angle.

Based on Figure 9, stability would be lowest on tooth 1, the one that cuts the throat region of the seat (see Figure 8) since the chip is heavily thinned due to its 70° lead angle. This is in agreement with the traditional size effect mindset. Since tooth 1 exhibits the lowest stability measure, it should be the target for improvement. However, there is more to the stability problem — the directional factor (see Eq. (10))

$$\frac{1}{\cos^2(\theta - \psi_r)}.$$

If the dominant dynamic mode is in the radial direction (θ = 90°), then tooth 1 becomes an even greater target since it is also the one that directs most of its thrust force into the radial (modal) direction. In other words, to get the complete stability picture one needs to scale the curves of Figure 9 by $1/\cos^2(90° - \psi_r)$, which provides a scaling of only 1.13 for tooth 1 compared to scaling values of 2 and 14.9 for teeth 2 and 3 with their respective 45° and 15° lead angles. On the other hand, if the dominant dynamic mode is in the axial direction, the curves of Figure 9 should be scaled by $1/\cos^2(0 - \psi_r)$ to see the full stability picture. These scaling factors are 8.55, 2 and 1.07 for teeth 1, 2 and 3, respectively.

It turns out that the directional factor dominates matters so that the worst tooth remains tooth 1 for θ = 90° but becomes tooth 3 for θ = 0°, as shown graphically in Figure 10 (tooth 3 stability for θ = 90° ranges from 45 to 110, so it is not shown). The percent improvement in stability gained with each edge preparation, relative to the baseline tool (solid circles in the plots), is independent of directional factor (i.e., θ) since each tooth experiences the same directional-factor scaling, independent of the edge prep. Based on these results (see right-hand plot of Figure 10 for convenience), the stability contributions of teeth 2 and 3 can each be improved by more than 100% by switching to a 100 μm x 10° chamfer. Switching to that same edge prep for tooth 1 would provide only a 50% improvement to the tooth-1 stability contribution. On the other hand, the stability contribution of tooth 1 could be increased by about 80% by switching to a 25 μm edge radius.

For comparison purposes, Figure 11 shows the stability measure as computed using the traditional power-law specific energy model. Here one would choose either a 5 μm or 25 μm

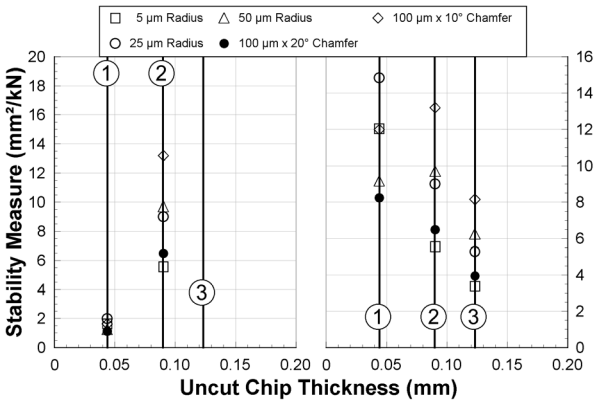

Figure 10 Stability measure for Material B, including directional factor: θ = 90° (left) and θ = 0° (right).

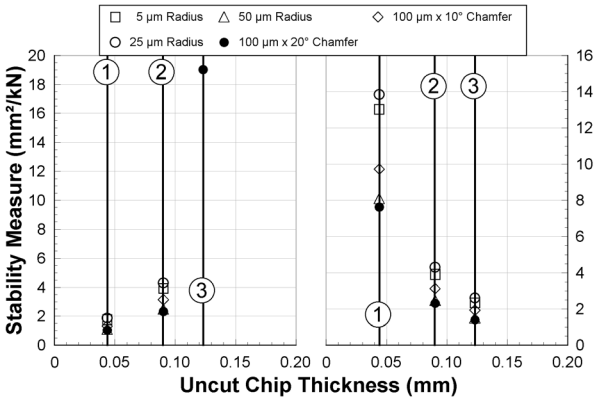

Figure 11 Stability measure for Material B, including directional factor, using the traditional specific energy power-law model: θ = 90° (left) and θ = 0° (right).

edge radius for tooth 1, expecting an 80% improvement over the baseline. Since the 25 μm edge radius provides better edge chipping resistance, as long as it does not produce unacceptable surface finish or residual stresses, it would be the preferred of the two. It turns out that for this particular feed rate, the uncut chip thickness on tooth 1 falls in a region of good accuracy for the 25-μm edge radius specific energy model, so that this recommendation and expected improvement are correct. By correct it is meant that this result matches the result derived from Figure 10, which is known to better represent the unit-force gradient and its effects on stability. However, the specific-energy model would misguide one into choosing that same 25 μm edge radius for teeth 2 and 3 expecting improvements of about 90% on each. On the contrary, the results derived from Figure 10

indicate that only a 40% improvement would be realized with the 25 μm edge radius as opposed to 2.5 times that improvement (> 100%) that would in fact be realized choosing the 100 μm x 10° chamfer.

5 CONCLUSIONS AND CONTINUING WORK

5.1 Conclusions

From the acquired force data, analysis of the computed gradients, and an exploration of candidate gradient models, the following hard conclusions can be drawn:

- The force gradient decays toward some finite positive value as uncut chip thickness becomes large. Some tool and work material combinations exhibit, based on the limited data here, a low-*h* drop-off in the unit-force gradient.
- The force gradient is not well captured using traditional model forms such as a power-law specific energy or second-order polynomial unit force, **even for gradients that exhibit a simple decay with increasing uncut chip thickness**. For simple decays, even at more 'conventional' (moderate to large) uncut chip thicknesses, gradient errors are ±25% **at best** and up to 100%, whereas force levels are typically predicted to within ± 20% **at worst**.
- A three-parameter exponential unit-force model provides a force-gradient fit that is consistently good, and improved compared to traditional model forms.
- Unit force is well predicted using the integral of the gradient model by identifying the integration constant from the force data as described.
- Tooling used for testing at a given edge preparation should be chosen (e.g., grade) so that a single edge can be used for all tests. Here, the carbide tooling was wearing extremely quickly compared to the CBN tooling used in production, requiring tool changes between each set of five *h*-levels. Slight changes in edge radius from edge to edge, not to mention wear progression, is an added source of noise in the replications.

One caveat of the exponential model proposed here does exist. That is, it requires substantially more than the two levels of uncut chip thickness commonly used to 'calibrate' the power-law specific energy model. Since increased testing is not desirable from a practical perspective, this need would further motivate the ongoing efforts to model edge preparation effects on forces using more sophisticated slip-line, upper-bound or FEA models. These more computational and complex models could then be used to rapidly generate many, many *h*-levels of force data to then be used to fit the semi-empirical model proposed here. The model proposed here, due to its relative simplicity and analytical form, is well suited to the analytical treatment of stability solutions whereas the more sophisticated mechanics-based models are not.

5.2 Continuing Work

The following is offered as an observation: the low-*h* drop-off in the unit-force gradient appears to be more prevalent when the edge radius becomes larger and for softer work materials. This statement is offered only as an observation. To raise this to a conclusion, further testing with more data in the low-*h* regime and for additional work materials would be needed for the following reasons:

- Despite the replication in the data here, the mere presence of the low-*h* drop-off could still be an artifact of experimental error, the effect of which being enhanced by the limited number of low-*h* levels (only 2 on each side of the drop off).
- The low-*h* drop-off, if it in fact does exist, would require more than two (hard and soft) materials to be tested to **conclude** a material-hardness effect.

Despite the obvious need for further testing, based on the intent of the study, it is considered successful and contributory as motivation to better understand the effects of edge preparation not only on force, but also on force gradient (stability). To reiterate, the intent of this work was to seek improved selection of edge preparation based on improving stability, all other process performance attributes such as surface finish and dimensional accuracy aside. Clearly, all performance attributes must be considered in selecting edge preparation and any other process condition. This study is intended to fill the 'stability performance' gap in that other efforts have focused on other performance attributes, such as force (dimensional accuracy), surface finish, tool wear, etc.

ACKNOWLEDGEMENTS

The authors gratefully acknowledge the support of Ford Motor Company AMTD and the involvement of other staff members, including

Drs. Richard Furness, Jon Johnson, Ed Exner and the machinist staff.

REFERENCES

[1] Knight, W. A., 1972, "Chatter in Turning: Some Effects of Tool Geometry and Cutting Conditions," *Int. J. Mach. Tool Des. Res.*, **12**, 201-220.

[2] Endres, W. J., 1996, "The Effect of Cutting Process Models, Process Gain Selection and Process Nonlinearity on Machining Stability Analysis," *Proc., Symp. on Physics of Mach. Processes – III*, ASME IMECE, 115-127.

[3] Beecherl, P., 2001, *Personal; Comm.*, Lamb Technicon Machining Systems, Research and New Product Development.

[4] Ozdoganlar, O. B., Endres, W. J., 1998, "An Analytical Stability Solution for the Turning Process with Depth-Direction Dynamics and Corner-Radiused Tooling," *Proc., Symp. on Advances in Modeling, Monitoring, and Control of Machining Systems*, ASME IMECE, **DSC-64**, 511-518.

[5] Fu, H. J., DeVor, R. E., Kapoor, S. G., 1984, "A Mechanistic Model for the Prediction of the Force System in Face Milling Operations," *ASME J. of Engg. for Ind.*, **106**, 81-88.

[6] Subramani, G., Suvada, R., Kapoor, S. G., DeVor, R. E., Meingast, W., 1987, "A Model for the Prediction of Force System for Cylinder Boring Process," *Proc., NAMRC,* **15**, 439-446.

[7] Chandrasekharan, V., Kapoor, S. G., DeVor, R. E., 1993, "A Mechanistic Approach to Predicting the Cutting Forces in Drilling," *Proc., ASME Sym. on Machining of Advanced Composites*, *ASME WAM*, 33-51.

[8] Nigm, M. M., Sadek, M. M., Tobias, S. A., 1972, "Prediction of Dynamic Cutting Coefficients from Steady State Cutting Data," *Annals of the CIRP*, **21**, 97-98.

[9] Peters, J., Vanhereck, P., van Brussel, H., 1972, "The Measurement of the Dynamic Cutting Coefficient," *Annals of the CIRP*, **20**, 129-136.

[10] Jemielniak, K., 1992, "Modeling of Dynamic Cutting Coefficient in Three-Dimensional Cutting," *Int. J. Mach. Tools and Manuf.*, **32**, 509-519.

[11] Smith, S., Tlusty, J., 1990, "Update on High-Speed Milling Dynamics," *Trans. ASME*, Vol. **112**, 142-149.

[12] Sutherland, J. W., 1987, "A Dynamic Model of the Cutting Force System in the End Milling Process," Ph.D. Thesis, University of Illinois at Urbana-Champaign, Urbana, IL, USA.

[13] Corpus, W. T., Endres, W. J., 2000, "A High-Order Analytical Solution for the Added Stability Lobes in Intermittent Machining," *Proc., Symp. on Machining Processes*, **MED-11**, 871-878.

[14] Sabberwal, A. J. P., 1961, "Chip Section and Cutting Force During the Milling Operation," *Annals of the CIRP*, **10**, 197-203.

[15] Hanna, N. H., Tobias, S. A., 1974, "The Theory of Nonlinear Regenerative Chatter," *ASME J. Engg. for Ind.*, **96**, 247-255.

[16] Budak, E., Altintas, Y., 1995, "Analytical Prediction of Chatter Stability in Milling – Part I: General Formulation," ASME, **DSC-57-1**, 545-554.

[17] Ozdoganlar, O. B., Endres, W. J., 1997, "A Structured Fully-Analytical Approach to Multi-Degree-of-Freedom Time-Invariant Stability Analysis for Machining," *Proc., Symp. on Predictable Modeling in Metal Cutting as Means of Bridging Gap Between Theory and Practice*, ASME IMECE, **MED-6-2**, 153-160.

[18] Tlusty, J., Polacek, M., 1963, "The Stability of the Machine Tool Against Self-Excited Vibrations in Machining," *ASME Prod. Engg. Res. Conf.*, Pittsburgh, 454-465.

[19] Ford, 2001, *Personal Communications and Internal Reports*, Ford Motor Company, Advanced Manufacturing Technology Development.